iScience, Volume *27*

Supplemental information

Voluntary wheel running improves molecular and functional deficits in a murine model of facioscapulohumeral muscular dystrophy

Adam J. Bittel, Daniel C. Bittel, Heather Gordish-Dressman, and Yi-Wen Chen

Supplemental Material

Supplemental Figures

Supplemental Figure 1. Body Weight & Muscle Weight – Related to Figure 1

A. Body weight (grams) measured at baseline, 3, and 6 weeks in all study groups (n=56, n=5 WT M Con, n=7 WT M Ex, n=6 WT F Con, n=6 WT F Ex, n=7 FLExDUX4 M Con, n=8 FLExDUX4 M Ex, n=9 FLExDUX4 F Con, n=8 FLExDUX4 F Ex, Three-way repeated measures ANOVA). '*' denotes overall, female mice had reduced body weight compared to male mice ($p<0.05$). See text for additional analyses of changes in body weight across groups. **B.** Muscle weight of the triceps brachii for mice in each group. '*' denotes overall, female mice had reduced triceps brachii muscle weights ($p<0.001$).

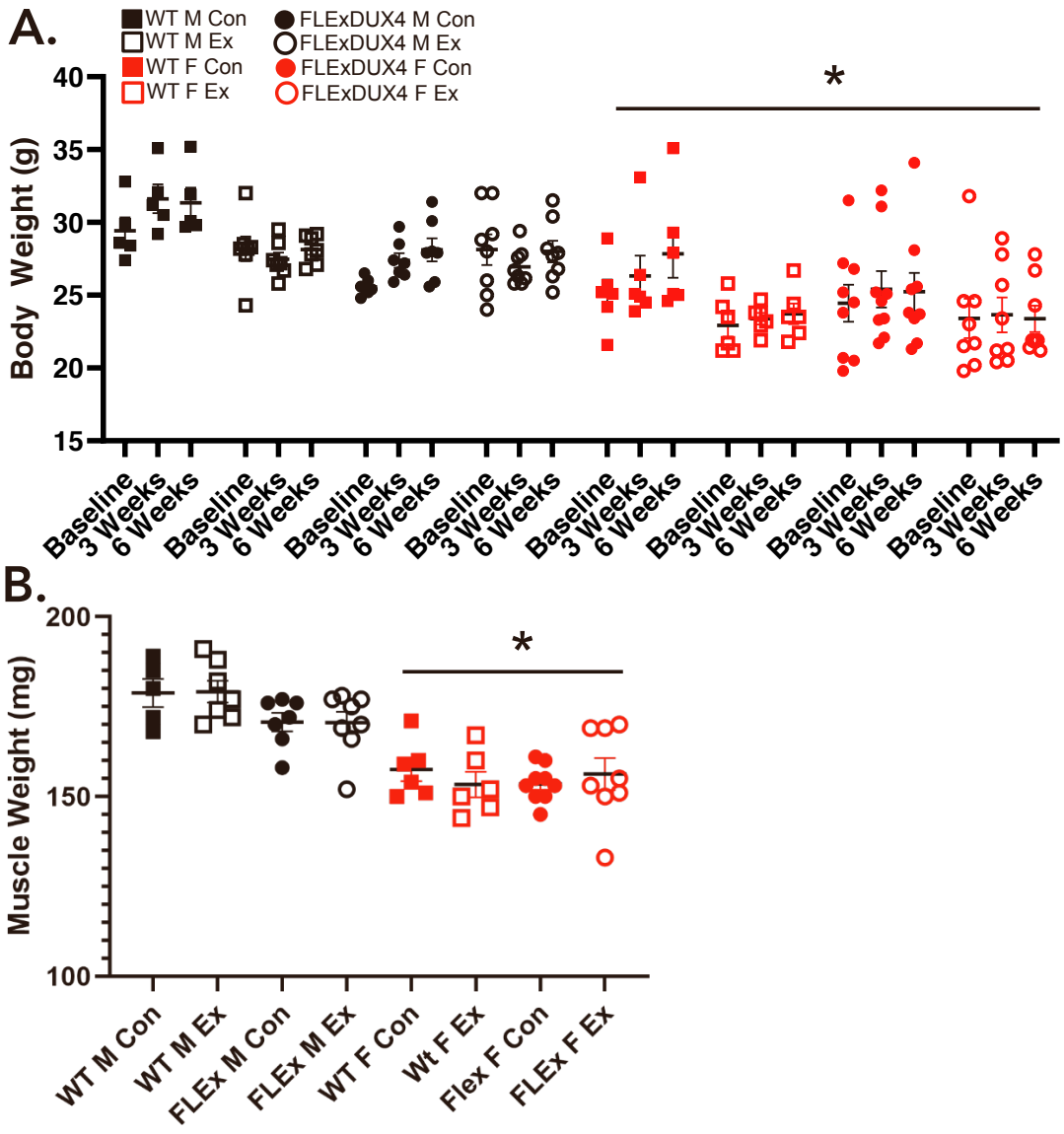

Supplemental Figure 2. Myofiber Cross Sectional Area – Related to Figure 2

Results of myofiber cross-sectional analysis. **A&B.** Distribution of fibers according to myofiber cross-sectional area (CSA, um^2) in male mice (A) and female mice (B) from control and trained groups. **C.** Average myofiber cross-sectional area for male and female mice in the control and exercise groups (n=50, n=5 WT M Con, n=7 WT M Ex, n=6 WT F Con, n=6 WT F Ex, n=8 FLExDUX4 M Con, n=6 FLExDUX4 M Ex, n=4 FLExDUX4 F Con, n=7 FLExDUX4 F Ex, three-way ANOVA). '*' denotes significant main effect of training status, with trained mice having significantly reduced myofiber cross-sectional areas vs un-trained control mice ($p<0.05$). '‡' denotes main effect of sex, with female mice having significantly reduced mean myofiber CSA vs male mice ($p<0.05$)

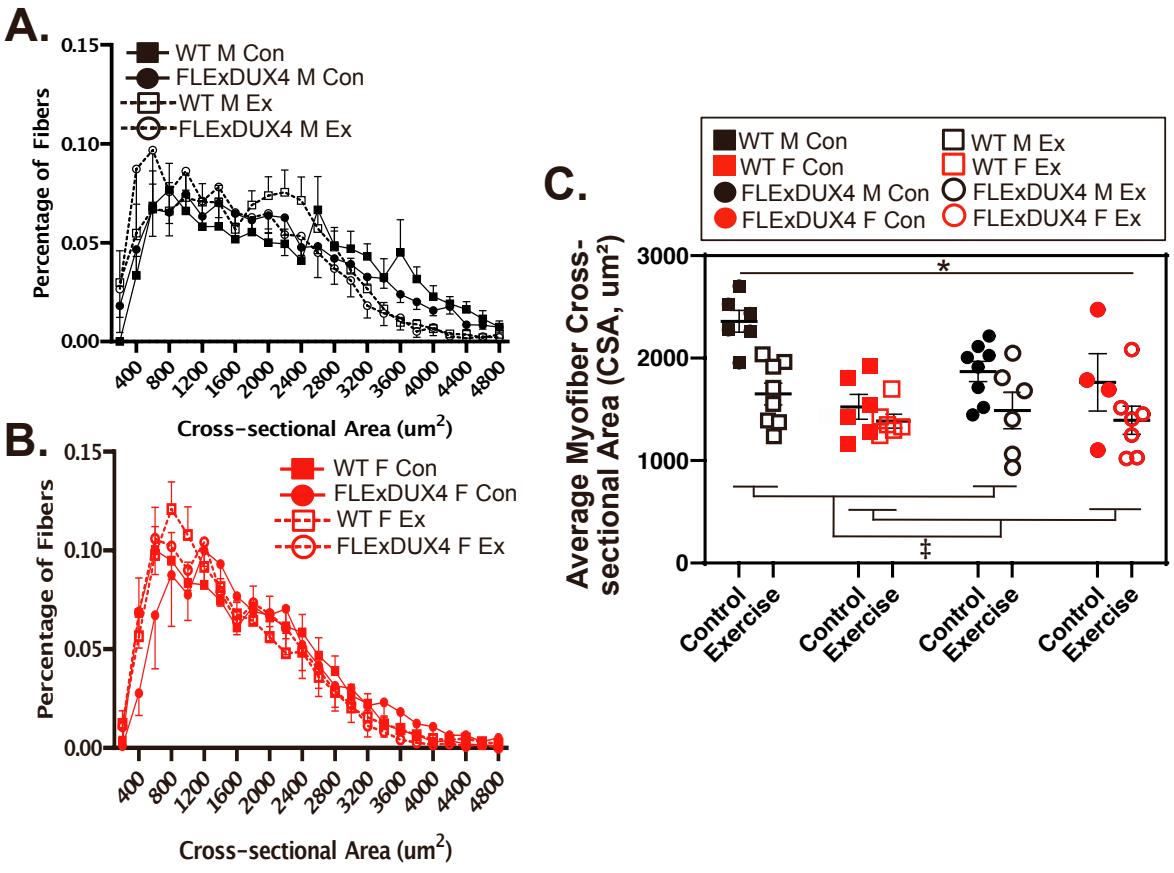

Supplemental Figure 3. Transcriptional Differences at Baseline and in Response to Exercise – Related to Figure 3

A. Chord diagram showing the proportion of differentially expressed genes (DEG, $p<0.01$) shared between the five main group comparisons (n=14, n=3 WT M Con, n=4 WT M Ex, n=3 FLExDUX4 M Con, n=4 FLExDUX4 M Ex). **B.** Volcano plot depicting predicted activation of significant (|z-score|>2, FDR $p<0.1$) IPA-identified upstream regulators of the transcriptional differences between FLExDUX4 Con and WT Con mice. Red = activated, green = inhibited. The top 15 regulators according to FDR p-value are labeled. **C.** Volcano plot depicting IPA-identified upstream regulators of DEG between FLExDUX4 Ex and WT Con mice, as in B. **D.** Dot plots depicting the top 10 significantly enriched gene ontologies among upregulated (left, red) and downregulated (right, green) DEG between FLExDUX4 Ex and WT Ex mice. Dots are colored according to their FDR p-value, and sized according to the number of genes from our dataset belonging to that gene ontology. **E.** Top 18 significantly enriched (FDR $p<0.05$) IPA canonical pathways among DEG between FLExDUX4 Ex and WT Ex mice. Bars are plotted according to $-\log_{10}$(FDR p-value) and colored according to their predicted activation z-score (green = downregulated pathways, red = upregulated, gray = no predicted z-score). **F.** Volcano plot depicting IPA upstream regulators of the transcriptional differences between FLExDUX4 Ex and WT Ex mice. Highly significant active/inhibited regulators are denoted by the red and green circles, respectively. The top 19 regulators according to FDR p-value are labeled.

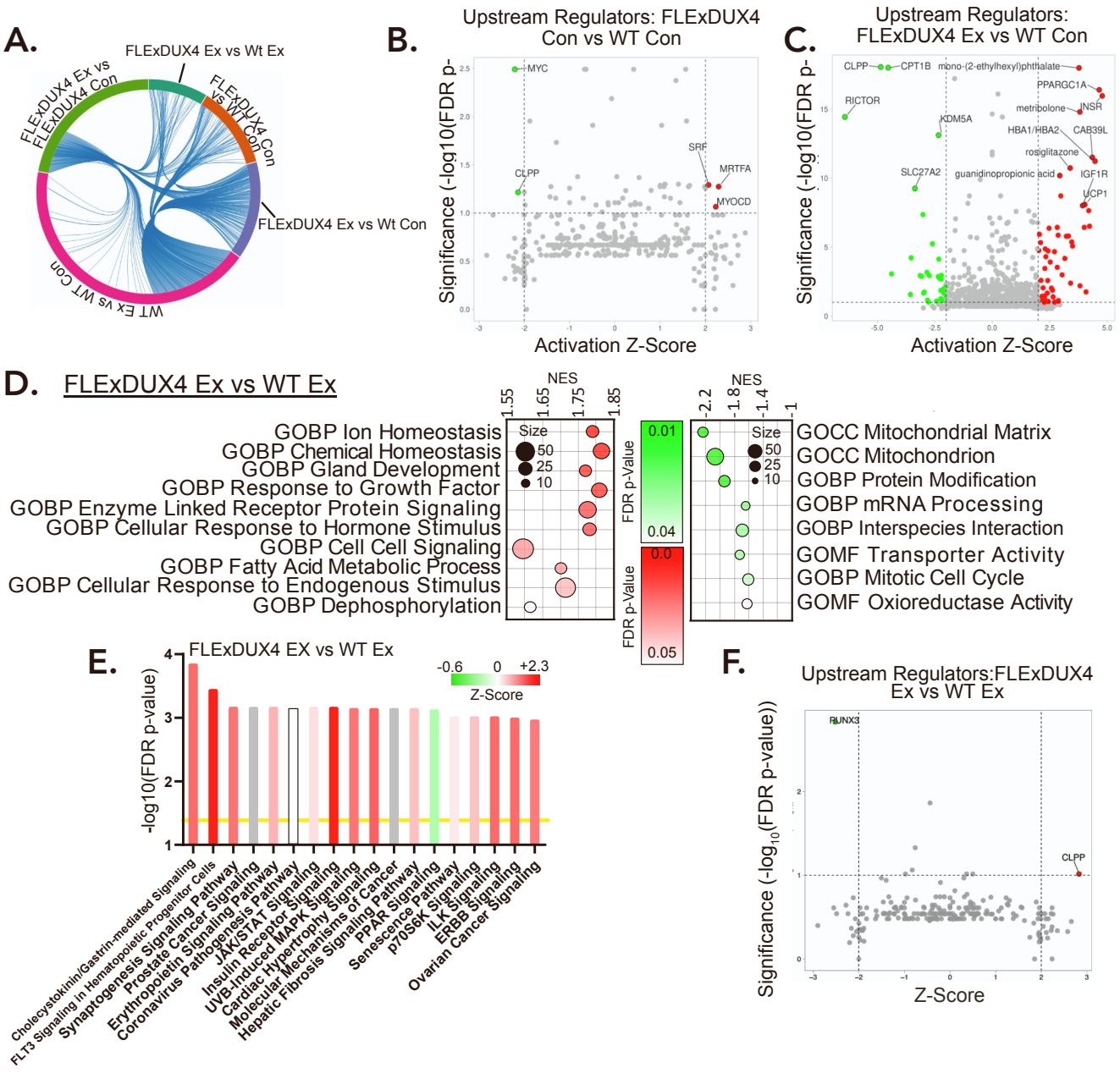
A.
FLExDUX4 Ex vs Wt Ex
FLExDUX4 Ex vs FLExDUX4 Con
FLExDUX4 Con vs WT Con
FLExDUX4 Ex vs Wt Con
WT Ex vs WT Con
B.
Upstream Regulators: FLExDUX4 Con vs WT Con
Significance (-log10(FDR p-
Activation Z-Score
MYC
CLPP
SRF
MRTFA
MYOCD
C.
Upstream Regulators: FLExDUX4 Ex vs WT Con
Significance (-log10(FDR p-
Activation Z-Score
CLPP
CPT1B
mono-(2-ethylhexyl)phthalate
PPARGC1A
RICTOR
metribolone
INSR
KDM5A
HBA1/HBA2
CAB39L
rosiglitazone
SLC27A2
guanidinopropionic acid
IGF1R
UCP1
D.
FLExDUX4 Ex vs WT Ex
NES
Size
50
25
10
FDR p-Value
0.01
0.04
0.0
0.05
GOBP Ion Homeostasis
GOBP Chemical Homeostasis
GOBP Gland Development
GOBP Response to Growth Factor
GOBP Enzyme Linked Receptor Protein Signaling
GOBP Cellular Response to Hormone Stimulus
GOBP Cell Cell Signaling
GOBP Fatty Acid Metabolic Process
GOBP Cellular Response to Endogenous Stimulus
GOBP Dephosphorylation
GOCC Mitochondrial Matrix
GOCC Mitochondrion
GOBP Protein Modification
GOBP mRNA Processing
GOBP Interspecies Interaction
GOMF Transporter Activity
GOBP Mitotic Cell Cycle
GOMF Oxioreductase Activity
E.
FLExDUX4 EX vs WT Ex
-log10(FDR p-value)
-0.6
0
+2.3
Z-Score
Cholecystokinin/Gastrin-mediated Signaling
FLT3 Signaling in Hematopoietic Progenitor Cells
Synaptogenesis Signaling Pathway
Prostate Cancer Signaling
Erythropoietin Signaling Pathway
Coronavirus Pathogenesis Pathway
JAK/STAT Signaling
Insulin Receptor Signaling
UVB-Induced MAPK Signaling
Cardiac Hypertrophy Signaling
Molecular Mechanisms of Cancer
Hepatic Fibrosis Signaling Pathway
PPAR Signaling
Senescence Pathway
p70S6K Signaling
ILK Signaling
ERBB Signaling
Ovarian Cancer Signaling
F.
Upstream Regulators:FLExDUX4 Ex vs WT Ex
Significance (-log10(FDR p-value))
Z-Score
RUNX3
CLPP

Supplemental Figure 4. Validation of RNAseq – Related to Figures 3 and 4

Results of the RNA sequencing validation using qRT-PCR. **A-E.** Plot of the log_2 fold change (log_2FC) in expression calculated from RNA sequencing and qRT-PCR for *ACTA2, EGLN3, MRPL4, PPARA, SOD2, TAB1, COX7A1*, and *PIM3* between (A) FLExDUX4 Con and WT Con groups; (B) FLExDUX4 Ex vs WT Con groups; (C) FLExDUX4 Ex vs FLExDUX4 Con groups; (D) WT Ex vs Wt Con groups; and (E) FLExDUX4 Ex vs WT Ex groups (n=14, n=3 WT M Con, n=4 WT M Ex, n=3 FLExDUX4 M Con, n=4 FLExDUX4 M Ex). Red bars denote the log_2FC calculated from RNA sequencing. Blue bars denote the log_2FC calculated from qRT-PCR. '*' denotes gene is significantly differently expressed between groups for RNAseq and/or qRT-PCR. F. Correlation with 95% confidence interval, and the coefficient of determination, between the log_2FC values calculated from RNA sequencing (x-axis), and qRT-PCR (y-axis).

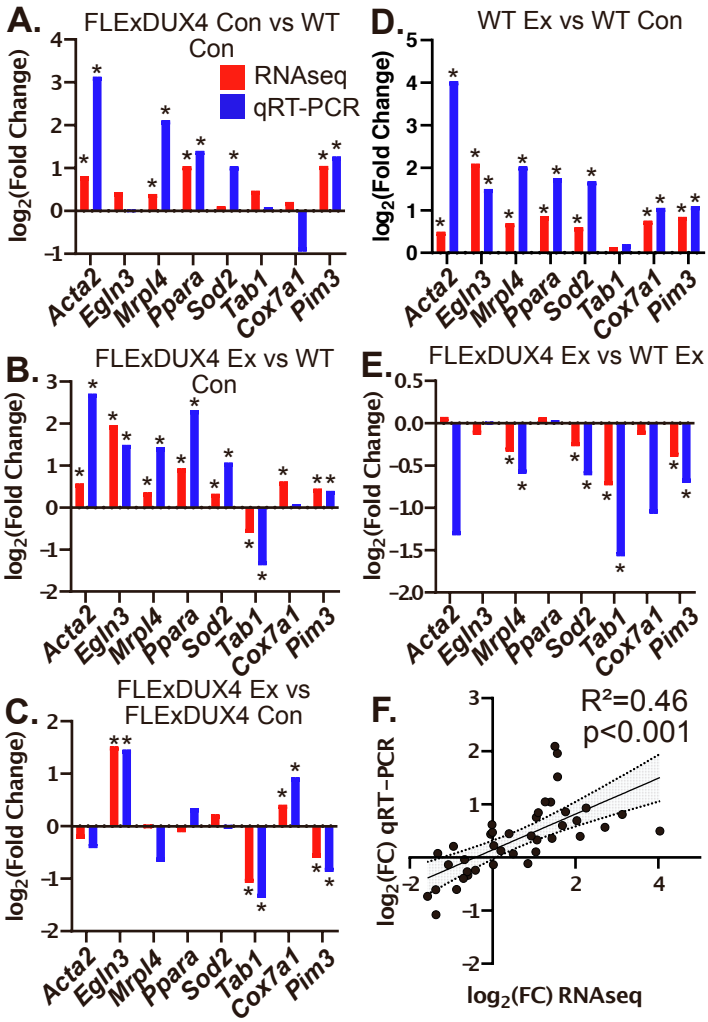

Supplemental Figure 5. Identification of the Most Significantly Differentially Expressed Genes Between Groups – Related to Figures 3 and 4

A-E. Volcano plots of genes identified in our RNAseq analysis for each of the five major study comparisons: FLExDUX4 Con vs WT Con (A), FLExDUX4 Ex vs WT Con (B), FLExDUX4 Ex vs FLExDUX4 Con (C), WT Ex vs WT Con (D), and FLExDUX4 Ex vs WT Ex (E) (n=14, n=3 WT M Con, n=4 WT M Ex, n=3 FLExDUX4 M Con, n=4 FLExDUX4 M Ex). Genes are plotted according to their log2FC (x-axis) and -$\log_{10}$(p-value). The most significantly differentially expressed genes are marked in color on each plot, based on |log2FC| > 1, and -log10(p-value) > 1.30, which corresponds to a canonical $p<0.05$. Green = downregulated, red = upregulated.

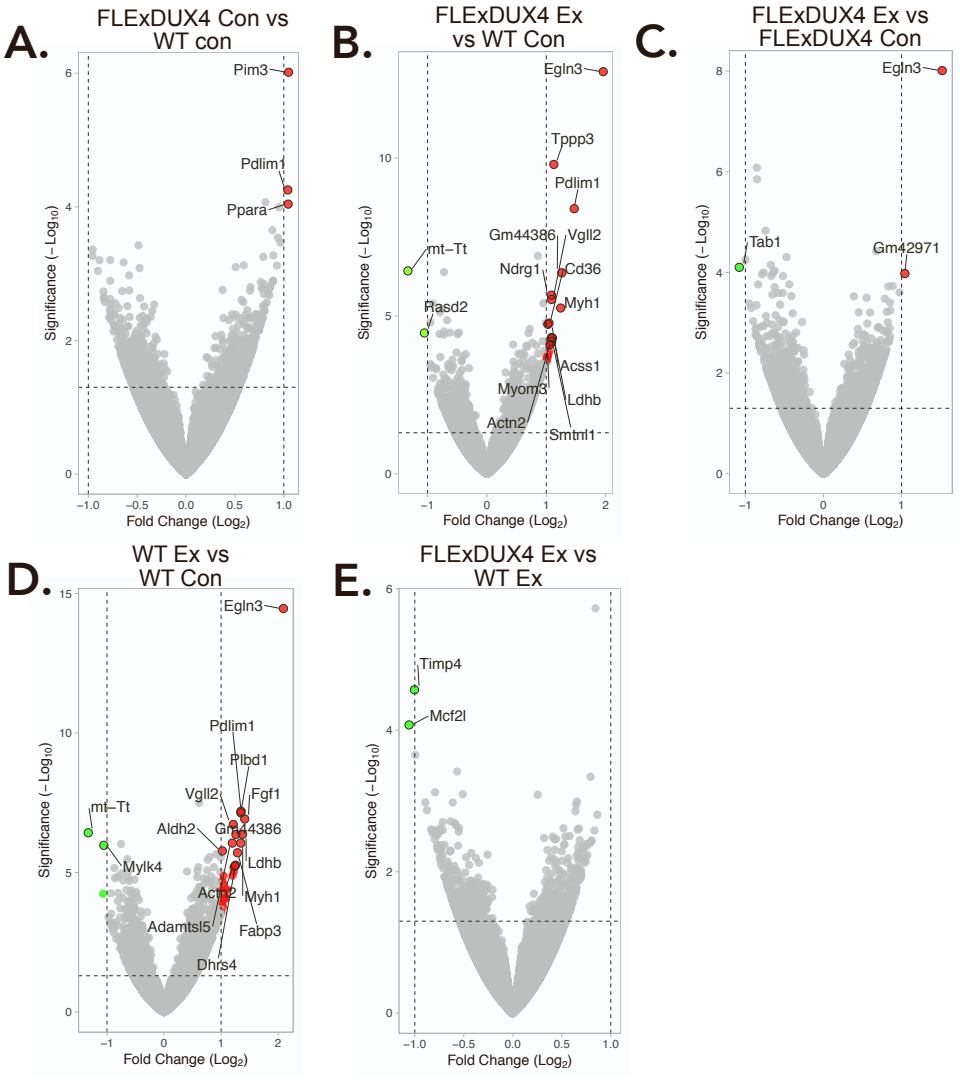

Supplemental Figure 6. Visualization of Group Transcriptional Heterogeneity Across Differentially Expressed Genes – Related to Figures 3 and 4

A. Heatmap of the expression of the top 500 DEG (|fold change| ≥ 1.5, p<0.05) across all four male study groups (n=14, n=3 WT M Con, n=4 WT M Ex, n=3 FLExDUX4 M Con, n=4 FLExDUX4 M Ex). Each column represents a single sample. Each row corresponds to one gene. Group identity is indicated by the black and white bars above the heatmap. **B-F**. Heatmaps depicting the expression of genes with |fold change| ≥ 1.5 and p<0.05 between FLExDUX4 Con vs WT Con (B), FLExDUX4 Ex vs WT Con (C), FLExDUX4 Ex vs FLExDUX4 Con (D), WT Ex vs WT Con (E), and FLExDUX4 Ex vs WT Ex (F). Hierarchical clustering was used to identify transcriptional similarities and group samples into similar clusters.

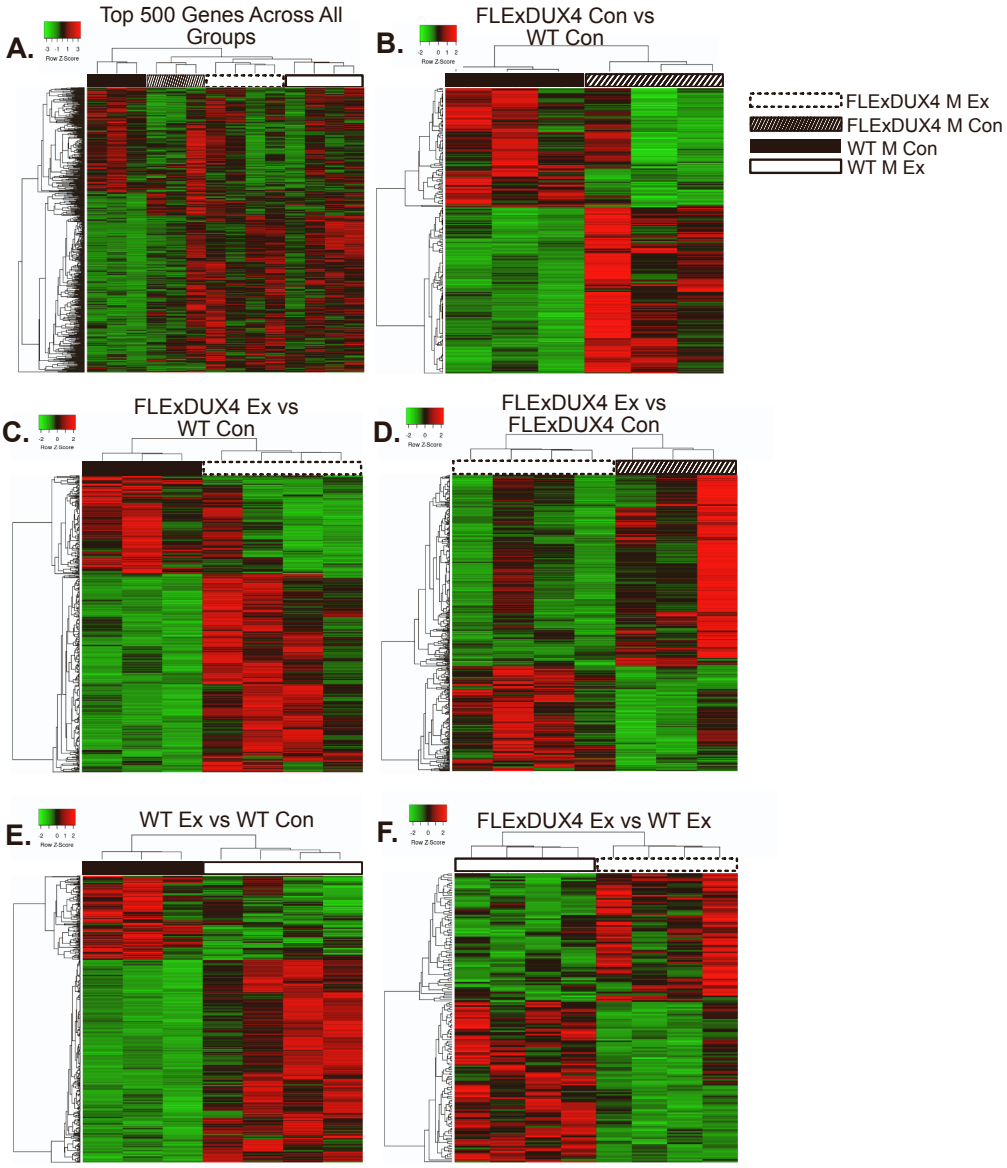

Supplemental Table 7. qRT-PCR and PCR primers – Related to STAR Methods

Gene	Forward	Reverse
Double Homeobox 4 (*DUX4*)	5′-CCCAGGTACCAGCAGACC-3′	5′-TCCAGGAGATGTAACTCTAATCCA -′
Mouse Glyceraldehyde-3-Phosphate Dehydrogenase (*Gapdh*)	5′-TTGTCAGCAATGCATCCTGC-3′	5′-CCGTTCAGCTCTGGGATGAC-3′
Mouse 16S Ribosomal RNA (*16S rRNA)*	5’-CCGCAAGGGAAAGATGAAAGAC-3’	5’-TCGTTTGGTTTCGGGGTTTC-3’
Mouse NADH:Ubiquinone oxidoreductase core subunit 1 (*Nd1*)	5’-CTAGCAGAAACAAACCGGGC-3’	5’-CCGGCTGCGTATTCTACGTT-3’
Mouse Hexokinase 2 (*Hk2*)	5’-GCCAGCCTCTCCTGATTTTAGTGT-3’	5’-GGGAACACAAAAGACCTCTTCTGG-3’
Mouse *Acta2*	5’-TGCTGACAGAGGCACCACTGAA-3’	5’-CAGTTGTACGTCCAGAGGCATAG-3’
Mouse *Egln3*	5’-CAGACCGCAGGAATCCACAT-3’	5’-TTCAGCATCGAAGTACCAGACAGT-3’
Mouse *Mrpl4*	5’-AGTCTCTCCGAGGCTTTGAGCA-3’	5’-CCTGAAGTTCCTCTGCCAGATG-3’
Mouse *Ppara*	5’-AGGCTGTAAGGGCTTCTTTCG-3’	5’-GGCATTTGTTCCGGTTCTTC-3’
Mouse *Sod2*	5’-TAACGCGCAGATCATGCAGCTG-3’	5’-AGGCTGAAGAGCGACCTGAGTT-3’
Mouse *Tab1*	5’-TTCCTGGTGCTGATGTCAGAGG-3’	5’-AGGTCTGCTTGGCAAACTCGGT-3’
Mouse *Cox7a1*	5’-AAACCGTGTGGCAGAGAAGCAG-3’	5’-CCCAAGCAGTATAAGCAGTAGGC-3’
Mouse *Pim3*	5’-TGTGGTCTCTGGGTGTACTGCT-3’	5’-GACACCACTCAATAAGCTGCTGG-3’
Genotyping Primer TJ76F	5’-CAATACCTTTCTGGGAGTTCTCTGCTGC-3’	
Genotyping Primer TJ77R	5’-CTCGTGTAGACAGAGCCTAGACAATTTGTTG-3’	
Genotyping Primer TJ78R	5’- TGCAGGACAACGCCCACACACC-3’	